Effect of Ionospheric Variability on the Electron Energy Spectrum produced from Incoherent Scatter Radar Measurements

Oliver Stalder
Björn Gustavsson

Institute of Physics and Technology,
UiT – The Arctic University, Tromsø, Norway

Abstract

The inversion of electron density profiles to electron energy spectra is performed for the first time with a fully dynamic ionospheric density model. Ion densities in the E-region may vary considerably during auroral precipitation [1], in particular the ratio of NO^+ and O_2^+, affecting the effective recombination rate. The comparison shows that due to the intense production of O_2^+ ions, the produced energy spectra are systematically shifted towards lower energies.

Method

The electron energy spectrum can be found from electron density profiles along the magnetic field, for example with the ElSpec algorithm [2]. The electron continuity equation is integrated, taking into account the altitude varying electron production q_e from auroral precipitation. Varying the parametrized differential number flux ϕ, affecting q_e, allows us to search for the best parameters for ϕ by fitting modelled electron density profiles to density profiles from radar measurements.

IonChem model

A model for ionospheric chemistry (IonChem) in the E-region was developed, taking into account relevant species and reactions between them. For every species, the continuity equation formulated, taking auroral production, recombination and chemical reactions into account:

$$\frac{dn_k}{dt} = q_k - l_k \qquad (1)$$

where the index k stands for different species, n is the density, q is production, and l are losses. The convective term $\nabla \cdot (n_k \boldsymbol{v}_k)$ is neglected. For electrons, production is due to auroral precipitation, and the production rate profile is linear in respect to the differential number flux ϕ [3, 4, 5]:

$$q_e = A\phi$$

Whereas losses are due to recombination:

$$l_e = \alpha_{eff} n_e^2$$

where α_{eff} is the effective recombination rate:

$$\alpha_{eff} = \frac{\alpha_{NO^+} n_{NO^+}}{n_e} + \frac{\alpha_{O_2^+} n_{O_2^+}}{n_e}$$

α_{NO^+} and $\alpha_{O_2^+}$ are the recombination rates of the respective ion species [6]:

$$\alpha_{NO^+} = 4.2 \cdot 10^{-13}\,(T_e/300)^{-0.39}\ \mathrm{m^3/s}$$

$$\alpha_{O_2^+} = 1.9 \cdot 10^{-13}\,(T_e/300)^{-0.5}\ \mathrm{m^3/s}$$

For ions, production and losses are due to chemical reactions, in the form of

$$\pm \alpha\, nk\, nj$$

with α being the reaction rate. Ions of major neutral species (N_2^+, O_2^+ and O^+) have also a production term proportional to the electron production. The system of coupled ordinary differential equations (ODE) described by Equation (1) is integrated using a stiff ODE solver to account for the large range of reaction rates.

Integration of IonChem with ElSpec

The IonChem model is then combined with ElSpec, performing the inversion based on the ionospheric densities and corresponding effective recombination rate. As the integration of the electron continuity equation requires solving the entire system of coupled ODE in IonChem, this becomes a computationally expensive operation. Instead, an iterative approach is adopted where the effective recombination rate, and thereby the ionospheric composition is assumed constant. A production rate profile is found, and used in IonChem to find updated ionospheric densities and effective recombination rate. These are then used to start the next iteration i of ElSpec.

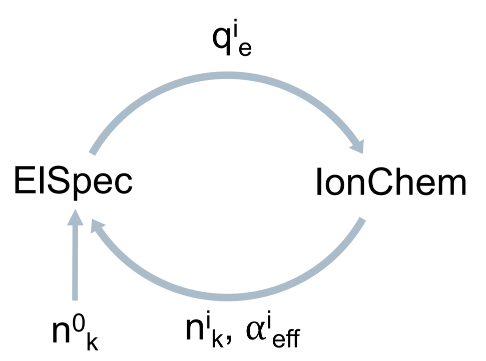

Over the course of a few iterations, a converging solution is found. The solution may not be unique. Therefore, different starting conditions have been investigated. We find that generally, the ionospheric densities converge to similar levels, independent of starting conditions.

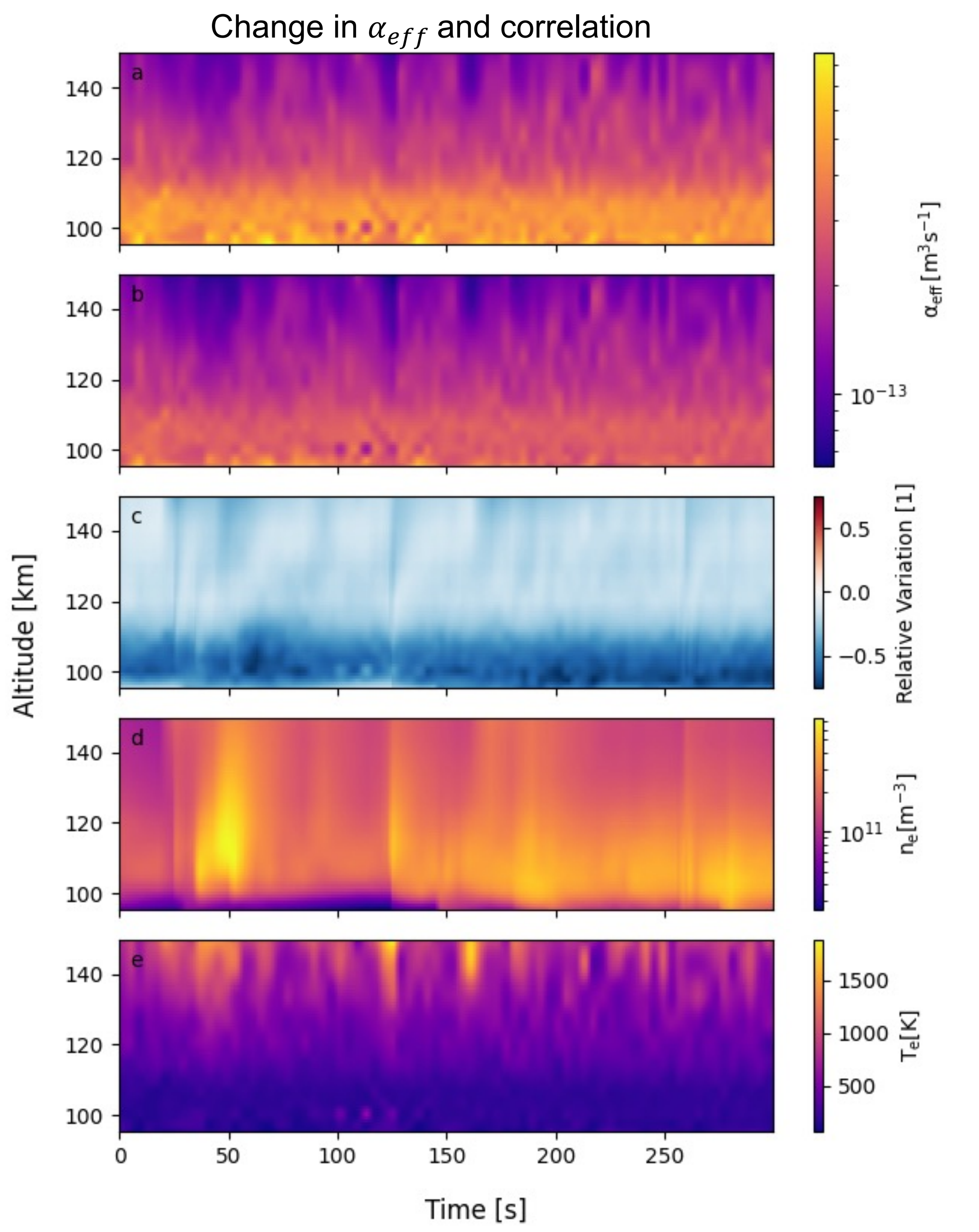

The difference in effective recombination rate and correlations with ionospheric parameters is shown. In panel a, the effective recombination rate the ElSpec is initialized with is shown. Panel b shoes the effective recombination rate after convergence A noticeable drop, especially at heights below 120 km can be observed. Panel c shoes the relative difference between panel a and b, highlighting the decrease in the effective recombination rate. Panel d and e show the electron density and electron temperature, respectively. Both show clear correlations with the relative difference in the effective recombination rate.

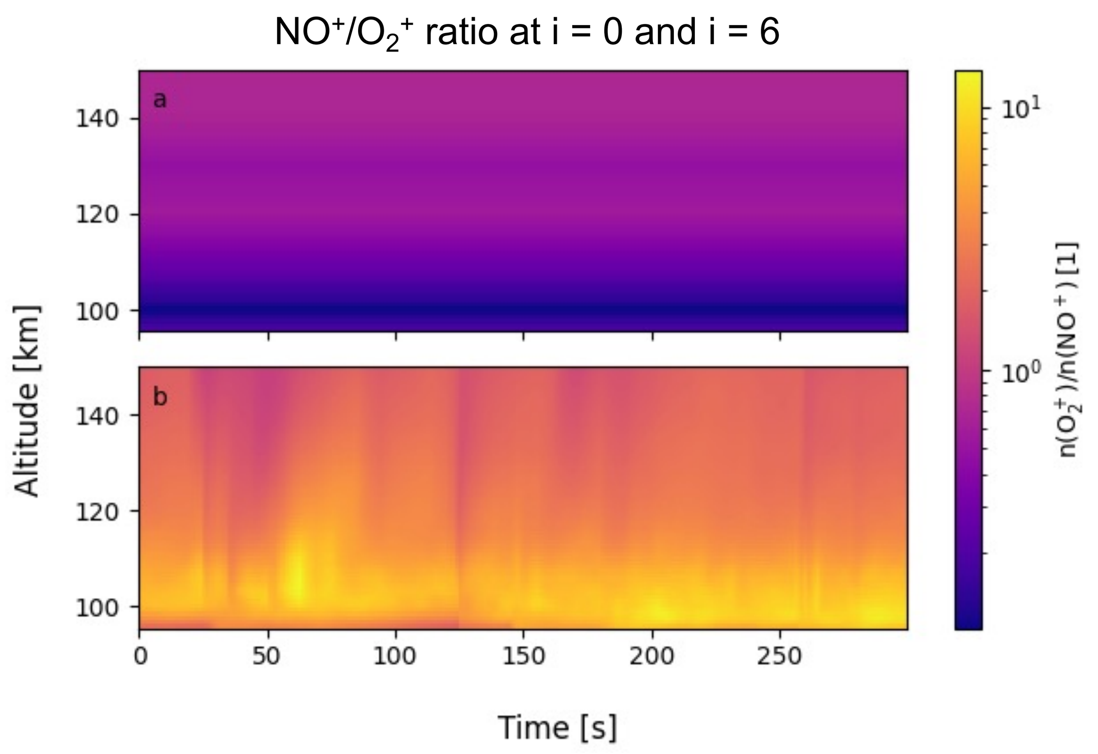

Panel a shows the initial NO^+/O_2^+ ratio, obtained from IRI. Panel b shows the NO^+/O_2^+ ratio after 6 iterations. Clearly visible is the variation introduced by IonChem. Furthermore, while the ratio is on the NO^+ side in the IRI model, the ratio is inverted in panel b, explaining the lower recombination rate in the figure above.

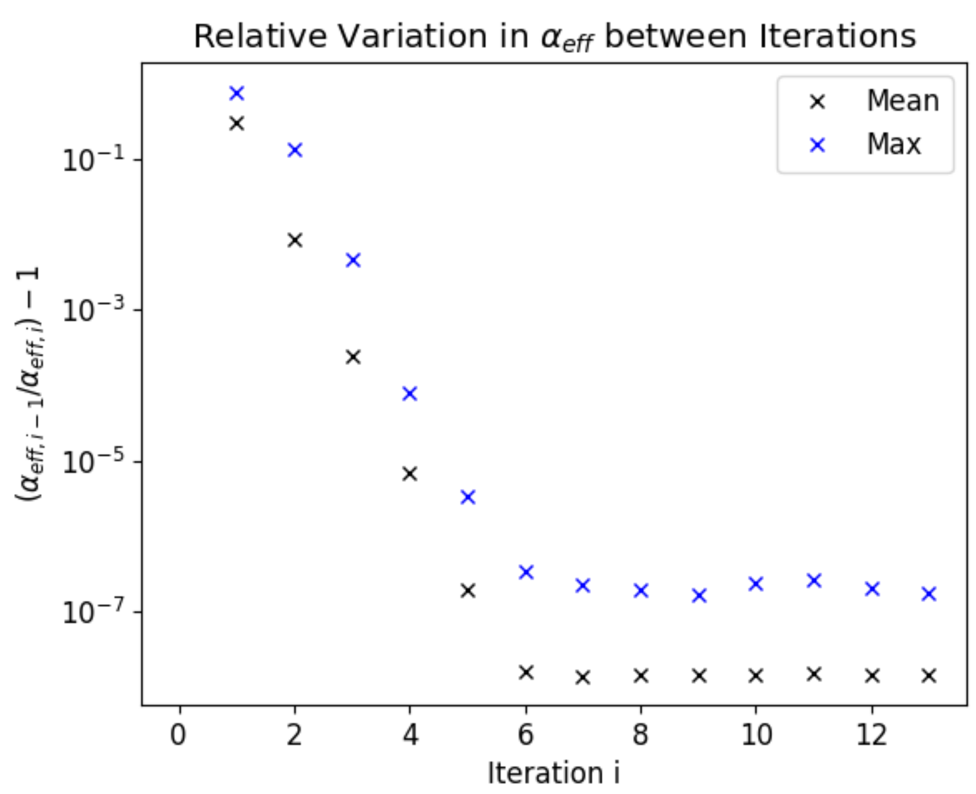

The convergence is investigated. Both mean and maximum relative variation in effective recombination rate over all height and altitude bins are decreasing monotonically until the 6th iteration. After that, they settle around a relative variation of 10^{-7}, corresponding to the relative accuracy of the employed ODE solver.

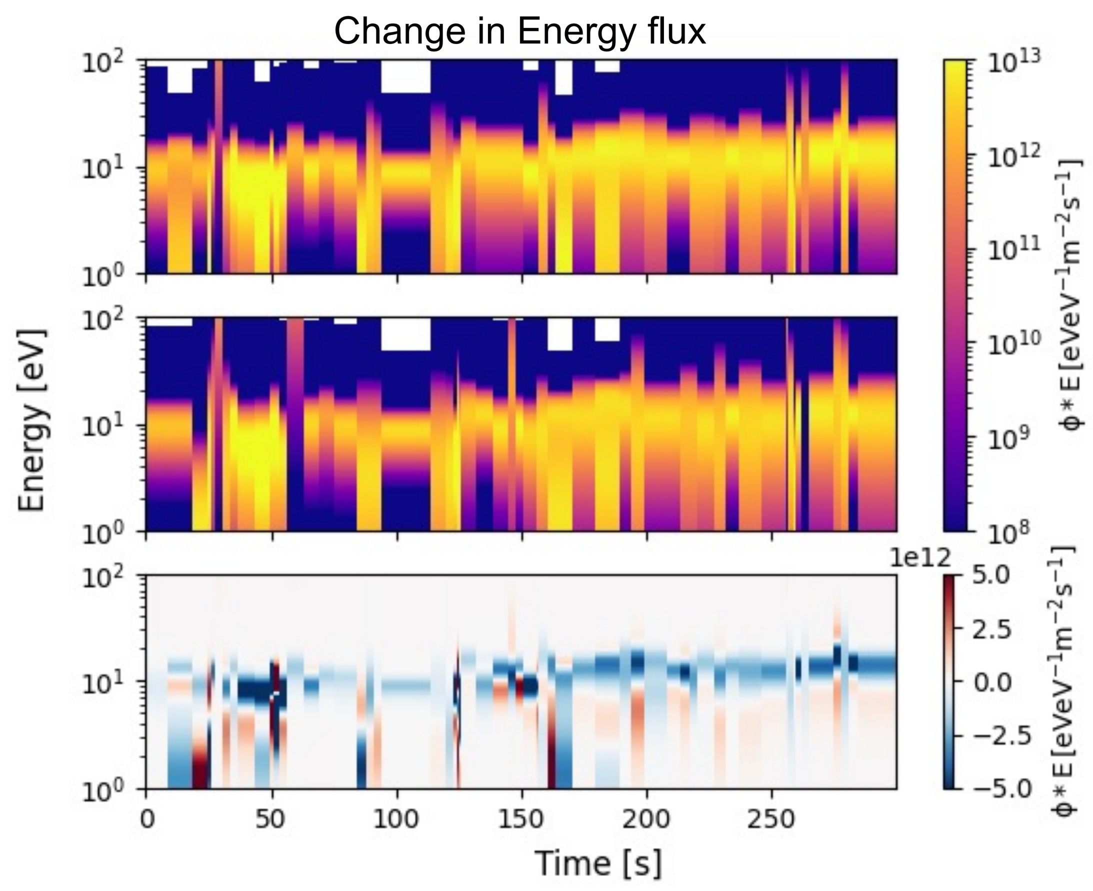

The effect of the diminished recombination rate on the differential energy spectrum is shown. The uppermost panel shows the differential energy spectrum after the initial run of ElSpec, and the middle panel shows is after the 6th iteration. As the differences are hard to discern, the lowest panel shows the differences between the two. Due to the diminished recombination rate, lower precipitation energy is needed to produce the same ionization, This can be seen as band of diminished flux at around 10 eV.

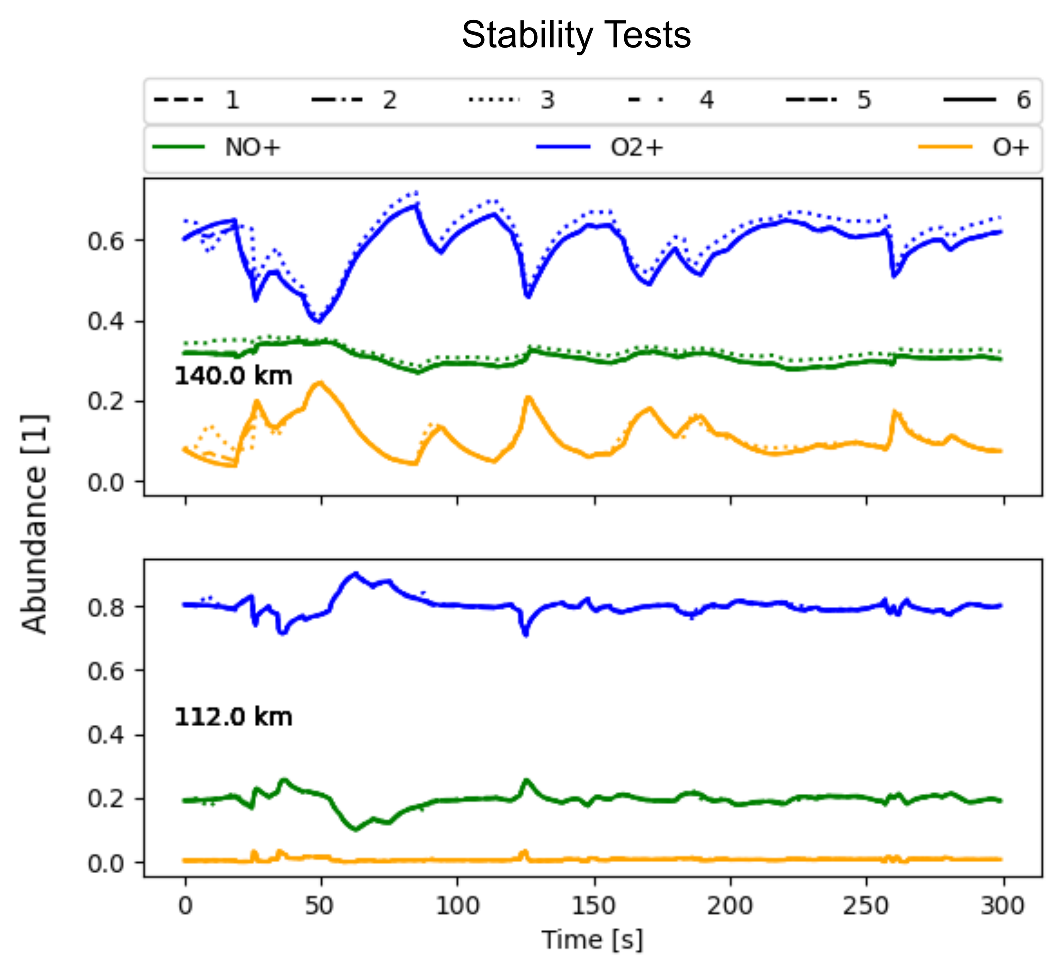

As the found solution may not be unique, some stability tests have been conducted. Starting off with different initial conditions, we investigate how the different results converge. The plot shows the densities of 3 different ions (NO^+, O_2^+ and O^+) for 6 different runs (in same order as in the plot):

1. A damped version, where variations in densities would be damped by a factor of 2 between iterations
2. Reversed NO^+/O_2^+ ratio, compared to IRI conditions
3. NO^+/O_2^+ ratio of 1, with no other ions
4. 3/10 in number density of NO^+, O_2^+ and O^+ ions each, and 1/10 N^+
5. 6/10 in number density of O_2^+, 3/10 of NO^+ and 1/10 of O^+
6. IRI conditions

All of the 6 runs show only minor deviations. Most notably, when starting with a NO^+/O_2^+ ratio of 1, both of them show increased levels at higher altitudes throughout the 5 minute window evaluated.

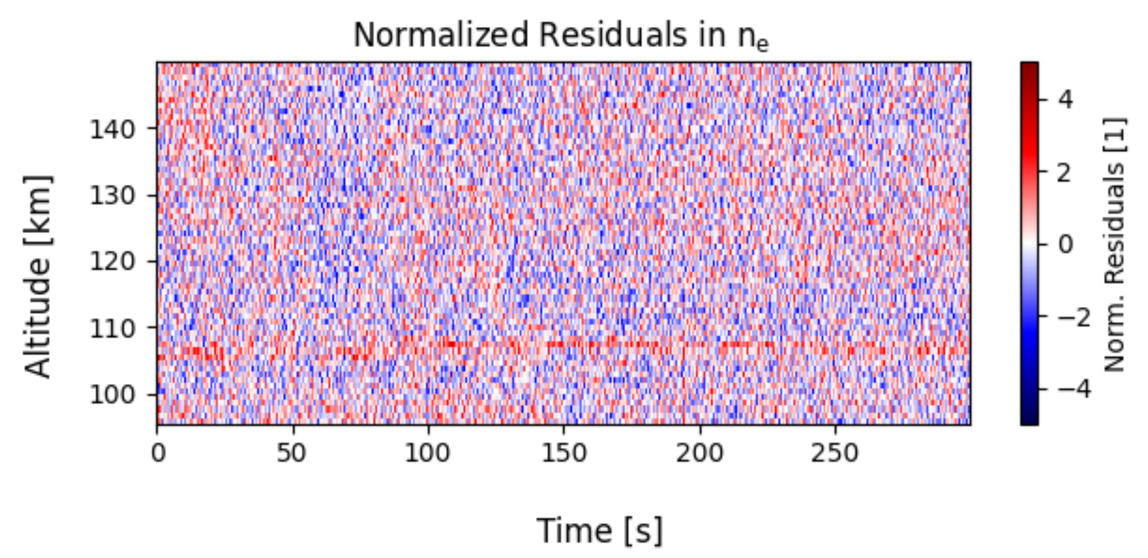

The difference between measured and modelled electron density is shown, normalized by the standart deviation of the measurements.

References:

[1] Jones, R. A., and M. H. Rees. "Time Dependent Studies of the Aurora—I. Ion Density and Composition." *Planetary and Space Science* 21, no. 4 (April 1, 1973): 537–57. https://doi.org/10.1016/0032-0633(73)90069-X.

[2] Virtanen, I. *et al*. "Electron Energy Spectrum and Auroral Power Estimation From Incoherent Scatter Radar Measurements." *Journal of Geophysical Research: Space Physics* 123, no. 8 (2018): 6865–87.

[3] Rees, M. H. *Physics and Chemistry of the Upper Atmosphere*. Cambridge Atmospheric and Space Science Series. Cambridge: Cambridge University Press, 1989. https://doi.org/10.1017/CBO9780511573118.

[4] Sergienko, Tima, and V. Ivanov. "A New Approach to Calculate the Excitation of Atmospheric Gases by Auroral Electrons." *Annales Geophysicae* 11 (January 1, 1993): 717–27.

[5] Fang, X. *et al* "Electron Impact Ionization: A New Parameterization for 100 EV to 1 MeV Electrons." *Journal of Geophysical Research: Space Physics* 113, no. A9 (2008). https://doi.org/10.1029/2008JA013384.

[6] Schunk, R., and Nagy, A.. *Ionospheres: Physics, Plasma Physics, and Chemistry*. 2nd ed. Cambridge Atmospheric and Space Science Series. Cambridge: Cambridge University Press, 2009.